Hindawi
Journal of Food Quality
Volume 2022, Article ID 3943052, 11 pages
https://doi.org/10.1155/2022/3943052

Research Article

Nontarget Metabolites of Rhizomes of Edible Sacred Lotus Provide New Insights into Rhizome Browning

Chenyang Hao,[1] Yuetong Yu,[1] Xueting Zhang,[1] Gangqiang Dong,[2] Yan Liu ,[1] and Sha Chen [1]

[1]*Key Laboratory of Beijing for Identification and Safety Evaluation of Chinese Medicine, Institute of Chinese Materia Medica, China Academy of Chinese Medical Sciences, No.16 Nanxiaojie Dongzhimennei, Beijing 100700, China*
[2]*Amway (China) Botanical R&D Centre, Wuxi 214115, China*

Correspondence should be addressed to Yan Liu; yliu1980@icmm.ac.cn and Sha Chen; schen@icmm.ac.cn

Received 16 June 2022; Revised 30 September 2022; Accepted 7 October 2022; Published 26 October 2022

Academic Editor: Addi Mohamed

The "edible rhizome" variant of *Nelumbo nucifera* with various cultivars has a long history of use as a food in East Asia. In this study, 48 target metabolites were untargeted and identified in 212 rhizome cultivars (tropical and temperate types) using ultraperformance liquid chromatography-electrospray ionization quadrupole time-of-flight high-resolution mass spectrometry; among these, 32 compounds were newly reported in the rhizome. Combined with the browning phenotype of 212 lotus rhizomes, (epi) catechin, norarmepavine, and *N*-feruloyl-3-methoxytyramine were used as predominant chemical markers to separate different degrees of lotus rhizome browning. *p*-Coumaroyltyramine and *N*-trans-feruloyltyramine were selected as predominant chemical markers to investigate the differential expression between tropical and temperate lotus using principal component analysis and orthogonal partial least squares discriminant analysis. Shared and unique structure plots were used to compare the outcomes of the ecotype and browning OPLS model, showing that variation in tropical lotus rhizome browning is not obvious; this will be of great importance for genetic improvement by providing a hereditary basis.

1. Introduction

Rhizomes (sacred lotus root) of the "edible lotus" variant of *Nelumbo nucifera* have been widely used as vegetables for thousands of years in China, South Korea, and Japan and are considered to be a nutritional food rich in carbohydrates, sugar, and several minerals [1, 2]. Based on ecotype, the lotus is classified into two types: temperate and tropical lotus [3]. Temperate lotus is distributed in the region north of 43° north latitude, and most of them are rhizomes. In contrast, tropical lotus is distributed in the region south of 13° south latitude, and most of them are flower lotus. Researchers have classified lotus in the 13°43° north latitude region subtropical lotus; however, a more scientific approach to ecological classification is needed in future investigations.

Several studies have demonstrated that lotus rhizomes possess antidiabetic, antioxidant, antipyretic, and antidiarrheal properties as they contain high levels of polyphenolic compounds [2, 4–6]. Metabolites produced by edible lotus rhizomes are used to prepare bread, cookies, and vegetable dishes. Browning can seriously affect the quality of fresh foods and processed products. However, there are no studies regarding the browning capacity of various lotus rhizomes and comparative metabolomic analyses among lotus cultivars. Rhizome usage is severely limited by its rapid browning and decline in quality after harvesting. Moreover, browning is one of the most important limitations in the storage and quality maintenance of lotus rhizomes [7]. Therefore, screening varieties with different browning abilities are of great significance for later directional breeding.

Browning of the rhizome can occur through enzymatic or nonenzymatic processes. The main process is enzymatic browning in which polyphenol oxidase catalyzes the conversion of phenols into o-quinones [8]. Polyphenols are compounds that are naturally synthesized during the secondary metabolism of plants; this process has attracted considerable attention from the scientific community because of the potential therapeutic effects of polyphenols [9].

Furthermore, phenolic compounds from fruits and vegetables are considered important because of their significant antioxidant activities [10, 11]. Morphological variations in rhizomes are reportedly associated with their genetic and physiological aspects involving secondary metabolites [9]. Therefore, wide phenotypic differences in genetic resources that favor chemical profile-based metabolomic approaches have been employed to distinguish different cultivars as well as metabolite biosyntheses. For example, studies have reported functional quality characterizations of cherry tomatoes and antioxidants with polyphenolic compounds in apples [12, 13].

Targeted metabolomics is a sensitive approach to measuring metabolites [14]. In most studies using low-resolution mass spectrometry (MS) instruments, such as ion-trap MS and triple-quadruple MS, it is not possible to determine the identities of the produced ions. Therefore, an ultra-performance liquid chromatography-electrospray ionization quadrupole time-of-flight high-resolution MS-based (UPLC-ESI-Q-TOF-HRMS) targeted metabolomics approach would be more suitable for exploring the quantified compounds and identifying the correlation between browning variations and chemical components.

In the present study, we selected 212 lotus cultivars of rhizomes that were planted in the same field to identify and quantify their comprehensive target metabolites and determine the relationship between browning and secondary metabolites using a UPLC-ESI-HRMS-based metabolomics approach. Our study aimed to comprehensively elucidate the untargeted chemical profiles in the rhizomes of lotus, investigate the differential metabolites of tropical and temperate lotus rhizomes, and use the orthogonal partial least square-discriminant analysis (OPLS-DA) model to separate different degrees of browning and screen important secondary metabolites that result in browning.

2. Materials and Methods

2.1. Chemicals and Reagents. Flavonoid standards catechin (MUST-14072210); gallocatechin (P27M11F114096); alkaloids armepavine (001299–202005) and nuciferine (W17N8Z48436); and the amino acids L-tyrosine (000828–202007), *N*-acetyl-D-phenylalanine (001560–202001), L-proline (000824–202003), L-phenylalanine (000837–202003), L-isoleucine (000825–202007), L-norleucine (001568–202007), L-asparagine (000829–202001), L-lysine (000834–202005), L-glutamic acid (000884–202009), L-histidine (001569–202008), L-arginine (000820–202003), L-glutamine (000830–202005), L-tryptophan (S07D7I26134), and L-methionine (000833–202006) were purchased from Shanghai Yuanye Biotechnology Co., Ltd. (Shanghai, China). The MS eluent and eluent additives of acetonitrile and formic acid were purchased from Sigma-Aldrich Corporation (St. Louis, MO, USA). Other analytical grade chemicals were obtained from Beijing Chemistry Factory (Beijing, China). Millipore membranes (0.22 μm) were purchased from Beijing Alltech Biological Products Co., Ltd. (Beijing, China). Ultrapure water was prepared using the Mill-Q SP system (Millipore Co., Bedford, MA, USA).

2.2. Plant Materials and Sample Preparation. To exclude the influence of the cultivation environment, all 212 *N. nucifera* (sacred lotus) cultivars were obtained from Wuhan Botanical Garden, Chinese Academy of Sciences, which were previously collected from Yunnan, Jiangsu, and Hubei provinces of Japan as well as Thailand [15]. Next, the rhizomes of each *N. nucifera* cultivars were cultivated in the United Lotus Germplasm Resource of the Amway Botanical Research Center (Wuxi, China) and the China Academy of Traditional Chinese Medicine (Beijing, China). All *N. nucifera* rhizomes were identified as *N. nucifera* Gaertn by professor Wei Sun, a taxonomist at the Institute of Chinese Materia Medica, China Academy of Chinese Medical Sciences in Beijing, China. They were cultivated in a laboratory field with a standard size (length 200 cm, width 100 cm) under the same conditions as observed in Wuxi, southern Jiangsu province (latitude, 31°57′N; longitude, 120°29′E). The rhizomes of the 212 cultivars were obtained in late November 2018. After 3 years of cultivation, mature rhizomes were randomly harvested from the pools. Information regarding the 212 cultivars is supplied in Supplementary Table 1, and the representative cultivar data, including browning and enlargement morphological variations, are summarized in Figure 1. Several parameters including L^* (lightness from black to white, scored 0 to 100), a^* (green or red color, ranging from a negative to positive value), and b^* (blue and yellow color, ranging from a negative to positive value) representing rhizome browning were measured using a spectrophotometer (NF555, Nippon Denshoku Industries Co., Ltd., Japan) (Table 1). The circumference (C) of the lotus root node and maximum swelling of lotus roots were measured using a micrometer.

Fresh rhizomes were obtained from each cultivar, and each rhizome was cut into 1 cm thick slices; they were immediately micro-dried in a ventilated oven at 100°C for 1 min and then at 45°C until they reached a constant weight. The dried rhizomes were powdered using an analytical mill (IKA A11 Basic Machine, Berlin, Germany) and stored at 4°C in the National Gene Bank of Traditional Chinese Medicine at the Institute of Chinese Materia Medica until their use for extraction and analysis. Two samples of different individuals were set as biological replicates, whereas two samples from the same individual that were extracted separately were considered technical replicates; all samples were analyzed in this study.

2.3. Preparation of Standard Solutions. All standards were accurately weighed and dissolved in methanol to obtain individual 1 mg/mL solutions, and the standard solutions were then diluted to achieve low (50 ng/mL), middle (100 ng/mL), and high (200 ng/mL) concentrations required for the preparation of quality control (QC) samples. "System suitability" was determined using QC samples, and the QC samples were injected after every ten experimental samples. These QC samples help determine the reproducibility and stability of the UPLC-ESI-Q-TOF-HRMS^n system.

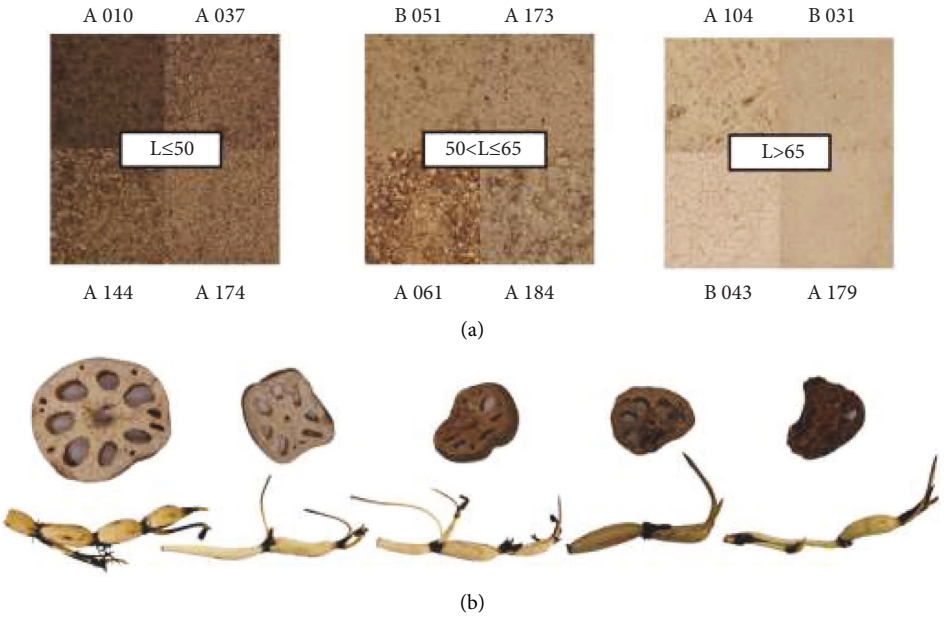

Figure 1: (a) Rhizomes of sacred lotus with different browning degrees, browning degree of 12 representative cultivars (BLXZ(A010), TH(A144), DFH1(A037), XZFC(A174), XFR2(B051), XJ(A173), HDL13(A061), YTJM(A184), MKBL(A104), LH(B043), 37(B031), and YCBL(A179)). (b) Representative samples of lotus root and corresponding slices of dried lotus root (AJN(A003), HXYR(A070), HWL(A073), JSWHO(A082), and JZLYP(A095)).

Table 1: Information on the browning of sacred lotus rhizomes.

No.	Name	Color	L	a^*	b^*	C	Variety
A010	BLXZ	Brown	27	9.664	15.16	10.8	Flower-lotus cultivars
A075	HWF	Brown	31.21	10.48	17.16	13.3	Flower-lotus cultivars
A056	GD	Brown	37.6	11.7	21.58	14.7	Flower-lotus cultivars
B002	Ti-13	Brown	38.14	10.55	22.25	8.3	Thai-lotus cultivars
A037	DFH	Brown	39.24	10.11	17.73	8.0	Flower-lotus cultivars
A138	SF	Brown	39.28	10.14	20.78	6.8	Flower-lotus cultivars
A151	WK7	Brown	40.01	11.24	22.99	12.0	Seed-lotus cultivars
A112	NHLL	Brown	40.72	9.352	18.54	12.2	Flower-lotus cultivars
A174	XZFC	Brown	41.37	10.03	23.57	11.4	Flower-lotus cultivars
A146	WZQH	Brown	43.5	8.805	20.54	6.2	Flower-lotus cultivars
A173	XJ	Khaki	50.25	8.281	20.48	8.2	Flower-lotus cultivars
A026	CHQY	Khaki	50.6	9.086	24.28	13.0	Flower-lotus cultivars
B051	XFR2	Khaki	52	7.453	16.53	8.1	Seed-lotus cultivars
A011	BSYL	Khaki	52.14	7.922	19.06	13.0	Flower-lotus cultivars
A016	BZGY	Khaki	52.14	7.922	19.06	10.3	Flower-lotus cultivars
A061	HDL13	Khaki	52.16	8.016	18.51	7.0	Flower-lotus cultivars
A141	TZTSL	Khaki	52.21	8.305	16.86	9.9	Flower-lotus cultivars
A162	XJL13A	Khaki	57.3	6.602	17.1	5.0	Flower-lotus cultivars
A184	YTJM	Khaki	60.06	5.25	16.45	9.4	Flower-lotus cultivars
A060	HDL	Khaki	60.1	7.016	16.55	10.0	Flower-lotus cultivars
A076	HY	Yellowish	65.53	4.18	16.37	10.0	Flower-lotus cultivars
B038	JX21	Yellowish	68.4	5.227	14.96	10.8	Seed-lotus cultivars
A179	YCBL	Yellowish	68.66	6.313	15.92	15.4	Flower-lotus cultivars
A177	YHL	Yellowish	68.75	5.117	15.46	10.2	Wild-lotus cultivars
B007	BJU	Yellowish	69.18	5.422	13.88	8.6	Flower-lotus cultivars
B032	BJ	Yellowish	69.27	5.82	14.02	10.0	Flower-lotus cultivars
A104	MKBL	Yellowish	70.42	4.273	15.08	17.3	Flower-lotus cultivars
B031	37	Yellowish	71.08	5.719[a]	12.24	23.0	Rhizome-lotus cultivars
B043	LH	Yellowish	71.44	5.594	12.75	14.9	Flower-lotus cultivars
B037	JNWM	Yellowish	75.61	4.57	11.1	19.7	Rhizome-lotus cultivars

a^*, green or red color, ranging from a negative to positive value. b^*, blue and yellow color, ranging from a negative to positive value. L, lightness from black to white, scored 0–100. C, circumference of the lotus root node.

2.4. Preparation of Sample Solutions. Each sample was extracted using 5 mL of 60% methanol acetic acid water (methanol: acetic acid: water: 60 : 40 : 1, v/v/v; pH 3.5) and treated ultrasonically for 40 min at 25°C; 1 g of each rhizome powder was accurately weighed. The extraction of each sample was performed twice. Subsequently, the sample was centrifuged at 8,000 × g for 5 min. The methanol solution was filtered through a 0.22 μm Millipore filter (Alltech Scientific Corporation) before performing liquid chromatography (LC-MS) analysis.

2.5. UPLC-ESI-Q-TOF-HRMS^n Conditions. The Agilent UPLC 1290II system combined with a 6540 Q-TOF-HR mass spectrometer (Agilent Technologies, Santa Clara, CA, USA) was used to determine the accurate mass of the metabolites. Sample ionization was achieved in the positive and negative modes within the mass/charge (m/z) range of 50–1000. The ESI source operating parameters in the positive and negative ion modes and ESI-MS conditions were as follows: gas temperature, 325 C; gas flow, 5 L/min; nebulizer, 35 psig; sheath gas temperature, 350 C; and collision energy voltage, 20 V (ESI+), 30 V (ESI+), and 40 V (ESI+). Internal references (purine and HP-0921) were used to modify the measured masses in real time. The reference masses in the positive ion mode ranged from m/z 121.0509 to m/z 922.0098, whereas they ranged from m/z 119.0363 to m/z 1033.9881 in the negative ion mode. The accurate molecular weight of each compound was used for quantification.

The UPLC equipped with a binary solvent delivery system, autosampler, and column compartment was used in this study. Chromatographic separation was performed on a Waters HLB C_{18} column, and the elution conditions were as follows: 0–15 min, 5% B; 15–20 min, 100% B. A and B indicate 0.4% acetic acid water (acetic acid: water, 0.4 : 100, v/v) and methanol, respectively.

2.6. Statistical Analysis. The *t*-test was used to analyze differences among groups via SPSS statistics (v.16.0, SPSS Inc.). A p value of <0.05 was selected to determine significant differences. Multivariate statistical analysis was performed using SIMCA-P (v.14.1, Umetrics, Umea, Sweden), in which the OPLS-DA model was used to identify markers. Hotelling' T^2 of 95% confidence interval is defined as the threshold of serious outliers in the principal component analysis (PCA) to exclude unusual samples. The OPLS-DA parameter R^2X represents the explanatory rate of the model to X matrices. R^2 indicates a measure of the model fit to the original data. Q^2 is an internal measure of consistency between the original and cross-validation predicted data. Differential metabolites were filtered using the results of variable importance for the projection (VIP) values.

3. Results and Discussion

3.1. Identification of Untargeted Metabolites in Lotus Rhizomes. Using UPLC-Q-TOF-HR-MS/MStechnology, metabolites in lotus root powder extracts were identified. We observed that the compounds showed increased response in the positive ion mode and were relatively abundant. Compare our data with those in the public database (MassBank and ChemSpider) and the 18 compounds that were identified by comparing their retention times, adduct ions, and product ions with those of authentic standards. A total of 48 compounds were identified in the positive or negative ion modes, which included 14 amino acids, 16 alkaloids, 5 nucleotide compounds, 2 flavonols, and 11 organic acids. Among these, 32 compounds (marked with ∗ in Table 2) were identified in lotus roots for the first time. The retention time and accurate m/z, of all qualitative compounds as well as their fragmentation information, are presented in Table 2.

The 48 compounds identified in 212 rhizomes of sacred lotus were quantitatively analyzed using untargeted UPLC-Q-TOF-HRMS/MS. Most of the identified compounds were investigated in the positive ion mode, except for compounds 14, 39, 41, 42, 47, and 48. All semiquantitative compounds identified in the 212 rhizomes of sacred lotus were used for subsequent analysis. Biological and technical replicates were used to ensure that reliable and high-quality data were acquired using the UPLC-Q-TOF-HR-MS-based untargeted metabolomics approach.

3.2. Multivariate PCA and OPLS-DA of the Population Structure. The browning of sacred lotus rhizomes varies highly among cultivars. In this study, the samples included 40 tropical and 172 temperate lotus cultivars. Tropical lotus cultivars mainly comprise flower lotus cultivars. Information regarding the cultivar is provided in Supplementary Table 1.

To evaluate the predominant metabolic profile differences between the two ecotypes, an unsupervised PCA approach was employed based on the information obtained via UPLC-Q-TOF-HRMS/MS analysis. Figure 2(a) shows the two-dimensional scatter plot of the PC1 versus PC2 score, which accounts for 35.2% of the total variance (19.4% and 15.8%, respectively). Rhizome samples of tropical and temperate lotus can be classified and identified based on metabolic profiles, which further demonstrated the low intraspecific variation in tropical lotus. However, the two clusters were not well defined and the predicted reliability of PCA (R^2X [cum] = 0.352, Q^2 [cum] = 0.137) was unsatisfactory.

The OPLS-DA model uses a supervised method for discriminating between models. OPLS-DA can separate predictive variation from orthogonal variation and enhance interpretation. Studies have shown that the separation between different groups of PCA scores is strongly associated with OPLS-DA cross-validation metrics. In this study, OPLS-DA was performed to enhance the sample separation observed in PCA analysis and identify the metabolites that provide the most relevant variables to discriminate between tropical and temperate lotus rhizome samples. For this model, the temperate lotus ecotype showed the most significant difference compared with the tropical lotus ecotype, and the statistic parameters of the model, i.e., R^2Y (0.823) and Q^2 (0.758) were found to be significant (Figure 2(b)). These metabolites are highlighted in red in the scatter plot

Table 2: Identification of target metabolites in rhizomes of sacred lotus.

No.	Type	Name	Rt	Mode	Molecular formula	Parent ion (m/z)	Error (ppm)	Secondary ion fragment (m/z) (relative abundance %)
1	Amino acids	L-Lysine	0.8	$[M+H]^+$	$C_6H_{14}N_2O_2$	147.1124	−2.72	84.0807 (100); 56.0501 (39.18)
2		L-Arginine	1.2	$[M+H]^+$	$C_6H_{14}N_4O_2$	175.1202	6.85	70.0659 (100); 60.0562 (24.63); 116.0711 (10.62); 130.0983 (8.97)
3		L-Asparagine	1.4	$[M+H]^+$	$C_4H_8N_2O_3$	133.0619	8.27	74.0241 (100); 70.0292 (11.73)
4*		L-Glutamine	1.4	$[M+H]^+$	$C_5H_{10}N_2O_3$	147.0765	0.68	84.0449 (100); 56.0502 (74.6);
5		L-Glutamic acid	1.4	$[M+H]^+$	$C_5H_9NO_4$	148.0606	1.35	84.0447 (100); 56.05 (97.69)
6		L-Methionine	1.5	$[M+H]^+$	$C_5H_{11}NO_2S$	150.0584	0.67	61.0111 (100); 56.05 (29)
7		L-Tyrosine	1.7	$[M+H]^+$	$C_9H_{11}NO_3$	182.0821	4.94	136.076 (100); 91.0548 (95.47); 119.05 (85.14); 123.0446 (78.48)
8		L-Norleucine	1.7	$[M+H]^+$	$C_6H_{13}NO_2$	132.1021	1.51	86.0963 (100); 69.0696 (11.38)
9		L-Isoleucine	1.8	$[M+H]^+$	$C_6H_{13}NO_2$	132.1023	3.03	86.0964 (100); 69.0701 (40.42)
10*		L-Glutimic acid	1.9	$[M+H]^+$	$C_5H_7NO_3$	130.0501	1.54	56.0499 (100); 84.0449 (69.91)
11		L-Proline	2.6	$[M+H]^+$	$C_5H_9NO_2$	116.0715	7.75	70.0632 (100); 100.094 (5.44); 68.0453 (6.39)
12		L-Phenylalanine	2.6	$[M+H]^+$	$C_9H_{11}NO_2$	166.0876	7.83	120.0819 (100); 103.0551 (21.77)
13		L-Tryptophan	3.9	$[M+H]^+$	$C_{11}H_{12}N_2O_2$	205.0969	−1.46	146.06 (100); 118.0651 (36.27); 144.0806 (27.71); 188.0703 (17.62)
14*		N-Acetyl-D-phenylalanine	7.4	$[M-H]^-$	$C_{11}H_{13}NO_3$	206.0792	−15.04	58.0234 (100); 162.8736 (27.81); 103.0427 (38.8); 100.9231 (35.66); 91.0451 (28.87)
15*	Alkaloids	N-Benzylidenemethylamine	2.6	$[M+H]^+$	C_8H_9N	120.0818	8.33	103.055 (100); 77.0395 (46.06)
16*		Coclaurine	3.2	$[M+H]^+$	$C_{17}H_{19}NO_3$	286.1436	−0.7	107.0485 (87.66); 255.101 (51.67); 161.0594 (31.5)
17*		N-Methylisococlaurine	3.7	$[M+H]^+$	$C_{18}H_{21}NO_3$	300.1593	−0.33	107.0486 (100); 143.0491 (29.83); 237.0899 (26.7); 137.0589 (25.93)
18*		N-Methylcoclaurine	4.0	$[M+H]^+$	$C_{18}H_{21}NO_3$	300.1594	0	107.049 (100); 237.0912 (16.08); 137.0617 (11.86); 269.1176 (9.57)
19*		Armepavine	5.0	$[M+H]^+$	$C_{19}H_{23}NO_3$	314.1776	7.96	283.1346 (100); 107.0501 (91.63)
20*		Norarmepavine	5.3	$[M+H]^+$	$C_{18}H_{21}NO3$	300.1614	6.66	107.0499 (100); 283.1343 (62.68); 268.1136 (29.18)
21*		Lirinidine	5.7	$[M+H]^+$	$C_{18}H_{19}NO_2$	282.1493	1.42	219.0803 (100); 251.1065 (98.48); 191.0853 (45.05)
22*		Caaverine	5.9	$[M+H]^+$	$C_{17}H_{17}NO_2$	268.135	6.71	191.086 (100); 251.1076 (93.94); 219.081 (90.13)
23*		Nuciferine	7.2	$[M+H]^+$	$C_{19}H_{21}NO_2$	296.1668	7.77	265.1241 (100); 250.1006 (51.18); 234.1042 (18.61)
24*		Roemerine	7.4	$[M+H]^+$	$C_{18}H_{17}NO_2$	280.1354	7.85	249.0928 (100); 219.0822 (16.36)
25*		(2Z)-N-[2-(3,4-Dihydroxyphenyl)-2-hydroxyethyl]-3-(4-methoxyphenyl)-2-propenamide	8.5	$[M+H]^+$	$C_{18}H_{19}NO_5$	330.1365	8.78	177.0559 (100); 145.0294 (20.88)
26*		p-Coumaroyltyramine	9.1	$[M+H]^+$	$C_{17}H_{17}NO_3$	284.1308	9.5	147.0452 (100); 121.0656 (47.76)
27*		Adenosine	9.2	$[M+H]^+$	$C_{18}H_{19}NO_4$	314.1389	0.64	177.0544 (100); 121.0644 (29.67); 145.0281 (19.77)
28*		N-Feruloyl-3-methoxytyramine	9.4	$[M+H]^+$	$C_{19}H_{21}NO_5$	344.1525	9.59	177.0561 (100); 145.0295 (15.55)
29*		(Â±)-Aegeline	10.6	$[M+H]^+$	$C_{18}H_{19}NO_3$	298.1443	1.68	131.0493 (100)
30*		Dehydrostephanine	13.1	$[M+H]^+$	$C_{19}H_{17}NO_3$	308.1308	8.76	249.0925 (100); 219.0816 (20.34); 191.0873 (7.86)
31	Nucleotides	Adenosine	2.0	$[M+H]^+$	$C_{10}H_{13}N_5O_4$	268.1055	5.59	136.0625 (100)
32*		Guanosine	2.3	$[M+H]^+$	$C_{10}H_{13}N_5O_5$	284.0993	1.41	152.0556 (100); 136.0725 (10.68)
33*		Adenosine 5′-monophosphate	3.4	$[M+H]^+$	$C_{10}H_{14}N_5O_7P$	348.0725	6.03	136.0627 (100)
34*		Succinyladenosine	4.3	$[M+H]^+$	$C_{14}H_{17}N_5O_8$	384.1153	0.78	252.0717 (100); 162.0769 (39.73); 192.0507 (22.66)
35*		5′-Deoxy-5′-(methylthio)adenosine	4.4	$[M+H]^+$	$C_{11}H_{15}N_5O_3S$	298.0988	6.71	192.0607 (100); 224.5401 (32.24); 136.1431 (6.7)
36	Flavanols	Gallocatechin	3.6	$[M+H]^+$	$C_{15}H_{14}O_7$	307.0834	7.16	139.0399 (100)
37		Catechin	5.1	$[M+H]^+$	$C_{15}H_{14}O_6$	291.0887	8.24	139.0401 (100); 123.0449 (52.38); 147.0454 (17.44)
38	Phenylpropanoids	Chlorogenic acid	5.1	$[M-H]^-$	$C_{16}H_{18}O_9$	353.0871	0.89	191.0555 (100)
39		Isoferulic acid	7.8	$[M-H]^-$	$C_{10}H_{10}O_4$	193.048	−13.47	134.0356 (100); 160.8392 (61.34); 135.038 (16.95)
40*		N-[2-Hydroxy-2-(4-hydroxyphenyl)ethyl]cinnamide	9.8	$[M+H]^+$	$C_{17}H_{17}NO_3$	284.1282	0.35	131.0492 (100); 137.0592 (12.1)

Table 2: Continued.

No.	Type	Name	Rt	Mode	Molecular formula	Parent ion (m/z)	Error (ppm)	Secondary ion fragment (m/z) (relative abundance %)
41*		Gluconic acid	1.3	$[M-H]^-$	$C_6H_{12}O_7$	195.0527	8.72	75.0099 (100); 59.0155 (53.2)
42*		L-Malic acid	1.7	$[M-H]^-$	$C_4H_6O_5$	133.013	−9.02	71.015 (100); 72.9945 (30.4); 59.0156 (7.8)
43*		Succinic acid	1.8	$[M-H]^-$	$C_4H_6O_4$	117.0196	2.56	73.0303 (100)
44*		Citric acid	2.0	$[M-H]^-$	$C_6H_8O_7$	191.0202	2.62	87.0086 (100); 111.0093 (85.8); 85.0302 (47.32)
45*	Organic acids	4-Acetamidobutyric acid	2.3	$[M+H]^+$	$C_6H_{11}NO_3$	146.0814	1.37	68.9972 (100); 86.0607 (51.2); 56.0501 (29.66)
46*		D-Pantothenic acid	3.8	$[M+H]^+$	$C_9H_{17}NO_5$	220.1193	6.36	90.0557 (100); 124.0764 (29.73); 202.1084 (11.79)
47*		2-Isopropylmalic acid	5.3	$[M-H]^-$	$C_7H_{12}O_5$	175.0587	−14.28	115.0388 (100); 203.9261 (84.5); 177.0164 (52.28)
48*		Azelaic acid	9.3	$[M-H]^-$	$C_9H_{16}O_4$	187.095	−13.9	57.0356 (100); 123.083 (96.94); 99.9262 (29.11); 97.0665 (75.39); 83.0508 (27.5); 80.0268 (40.6)

*Marked as the first identification from the rhizome of sacred lotus.

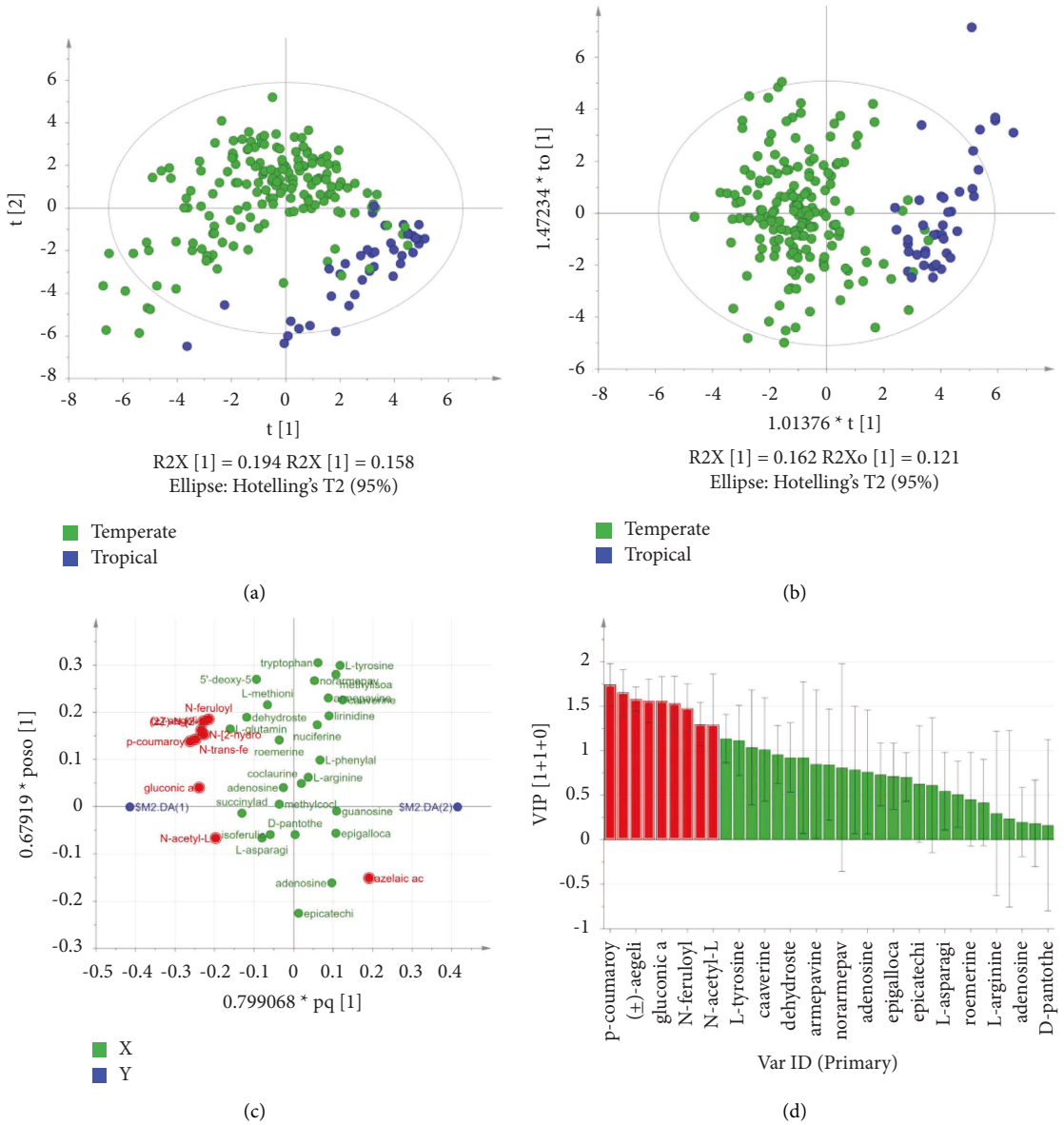

Figure 2: Relationship between secondary metabolites (polyphenols, amino acids, and alkaloids) and their ecotype in 212 sacred lotus rhizome cultivars (significant compounds are shown in red). (a) PCA score plot of 212 sacred lotus rhizomes with different ecotypes. (b) OPLS-DA score plot of 212 sacred lotus rhizome with different ecotypes. (c) S-plot of 48 identified and quantified compounds. (d) VIP distribution of the 48 identified and quantified compounds.

(S-plot) (Figure 2(c)) with VIP (Figure 2(d)) values of >1, which also satisfied the conditions $|p| > 0.1$ and $|p(\text{corr})| > 0.5$ in the destructive statistic list. They were considered potential metabolites for characterizing the chemical composition differences between tropical and temperate lotus rhizomes. The characteristic metabolites of the temperate lotus ecotype were *p*-coumaroyltyramine, (Â±)-aegeline, gluconic acid, *N*-feruloyl-3-methoxytyramine, and *N*-acetyl-L-phenylalanine and that of the tropical lotus ecotype was azelaic acid.

3.3. Association between Browning of Lotus Rhizome and Metabolites. The L^*, a^*, and b^* values of all the cultivars were 27.00–75.61, 4.18–11.7, and 11.1–24.28, respectively. The L^*, a^*, and b^* values of lotus rhizome samples were normally distributed. Browning of the lotus root can be well described because L^* values from low to high represent sample colors from black to white. To screen out metabolites associated with the browning of lotus roots, we categorized the lotus root samples into three groups based on the L value values: Group I (44 samples, $L \leq 50$), Group II (127 samples, L 50–65), and Group III (41 samples, $L \geq 65$). To determine the relationship between metabolites and browning, samples were plotted using PCA, which could provide an overview of the complete dataset, showing variability between browning or L value and metabolites. The PCA plot showed no clear separation of the three different L^* value groups, demonstrating that the L^* value is a continuous variable. However, samples with higher L values were distributed on the positive

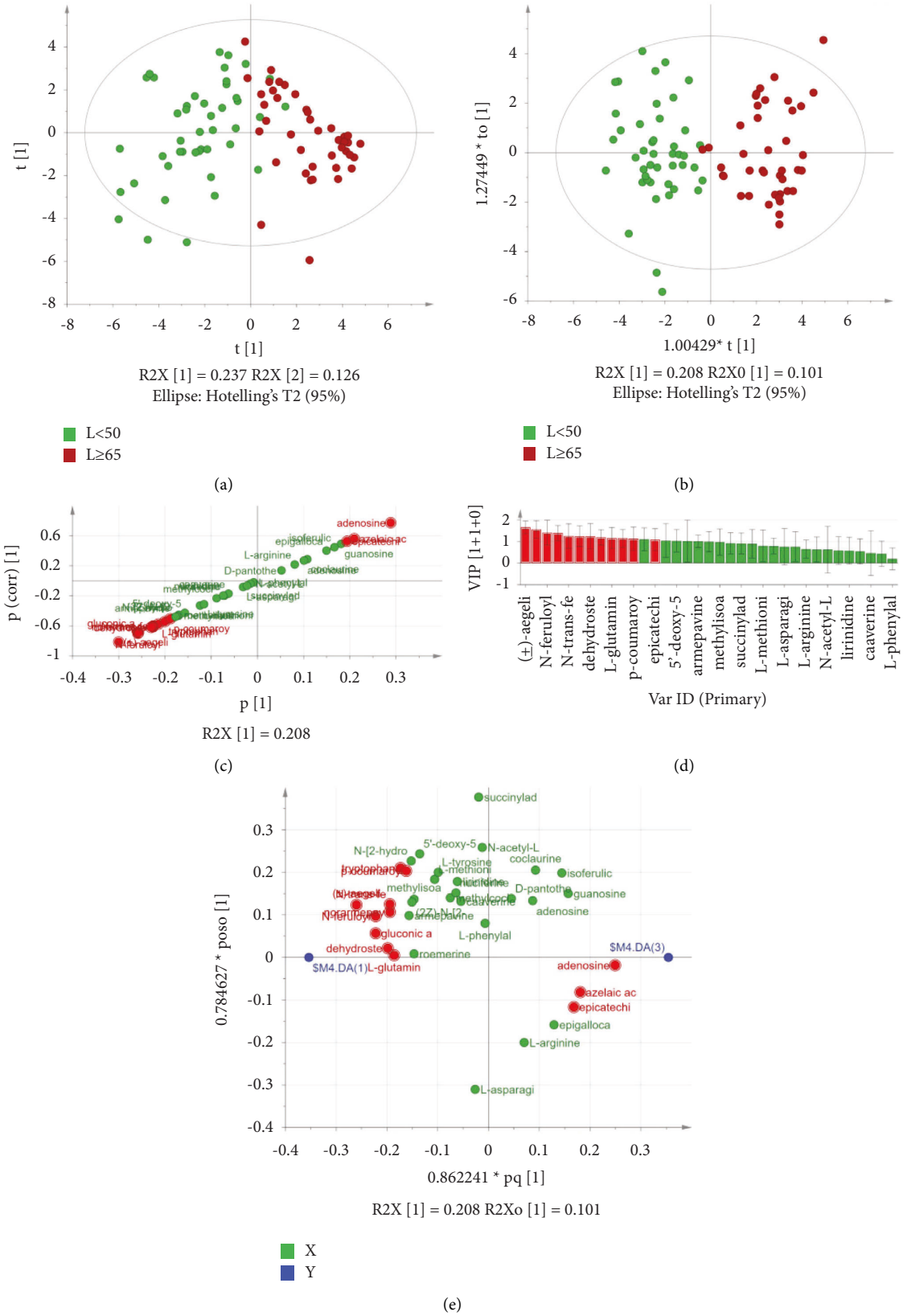

Figure 3: Relationship between targeted secondary metabolites (polyphenols, amino acids, and alkaloids) and their morphological variations (browning and size) in 212 sacred lotus rhizome cultivars (significant compounds are shown in red). (a) PCA of 212 sacred lotus rhizomes with different morphological variations. (b) OPLS-DA of 212 sacred lotus rhizomes with different morphological variations. (c) S-plots of secondary metabolites constructed using OPLS-DA analysis. (d) VIP distribution of the 48 identified and quantified compounds.

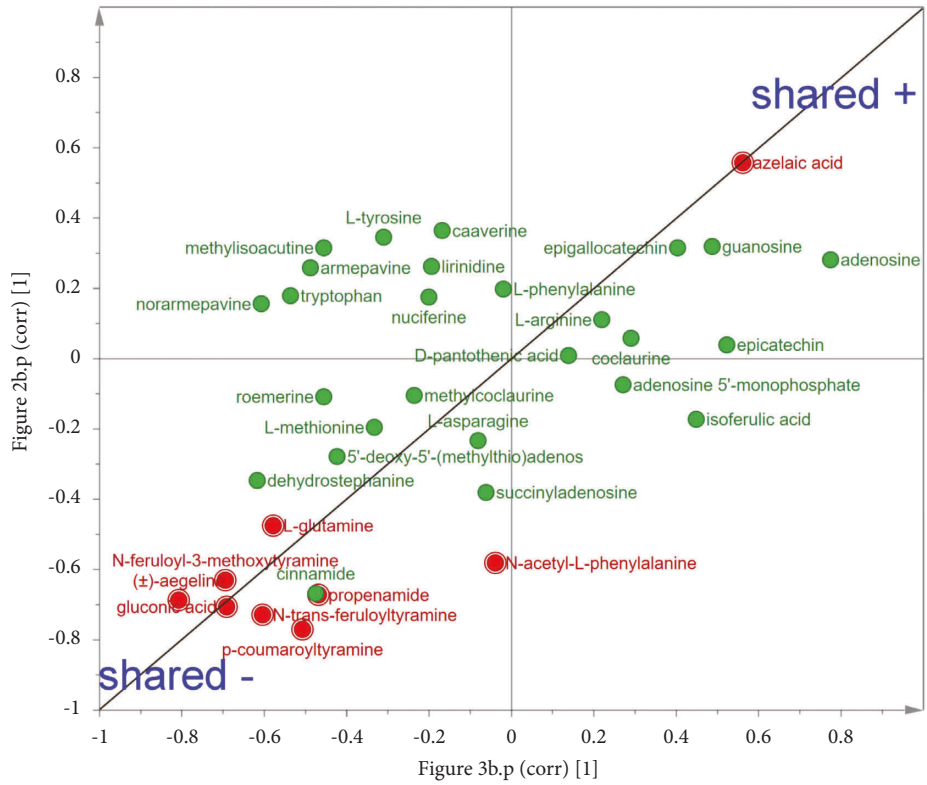

Figure 4: SUS-plot of two OPLS models (browning and ecotype classification).

part of the first principal component, whereas those with lower scores were distributed on the negative part of the first principal component. PCA analysis performed on the two groups revealed a clear separation of Group I ($L \leq 50$) and Group III ($L \geq 65$) along the PC1 axis. PCA on these attributes accounted for 36.3% of the variance, with 23.7% of PC1 and 12.6% of PC2 (Figure 3(a)). PCA scores space separation was the sole basis for obtaining effective OPLS-DA cross-validation metrics. Therefore, the two most outlying lotus root powder samples were subjected to OPLS_DA analysis, which can be used to calculate the response-related and orthogonal predictive variables.

The OPLS-DA score plots showed better separation between Groups I and III along *X*-axis. When browning was compared with metabolite concentration, strong reliability ($R^2Y = 0.823$, $Q^2 = 0.758$) of the OPLS-DA models was noted (Figure 3(b)). To identify the strong correlation between metabolite concentration and browning of lotus rhizome samples, three statistical tools, including S-plot, VIP, and loading plot, were used (Figures 3(c) and 3(d)). The S-plot showed a graphical interpretation of the covariance as well as the correlation between loading variables and predictive score *t* [1]. The *p* [1] axis is the visualization of contribution, whereas the *p*(corr) [1] axis spans between +1 and −1 as the correlation. Therefore, the *X*-variables were the farthest from the origin and had high influence and reliability. Compounds in the low *L*-values group were at higher levels than those in the high *L*-value group of lotus rhizome samples which mainly comprised alkaloids and amino acids, including (Â±)-aegeline, *N*-feruloyl-3-methoxytyramine, *N*-trans-feruloyltyramine, dehydrostephanine, L-glutamine, gluconic acid, norarmepavine, tryptophan, and p-coumaroyltyramine. Only a few metabolites, including (epi) catechin, azelaic acid, and adenosine, were at significantly higher levels in the high *L* value than in the low *L* value group.

3.4. SUS Based on the Browning and Ecotype OPLS-DA Models. To identify unique compounds between two separate different OPLS-DA models, the SUS-plot was used. If two OPLS models have similar profiles, the *X*-variables would line up along the diagonal, running from the lower-left corner to the upper-right corner, and form a scatter plot based on the *p* (corr) [1] vector from two separate OPLS models. OPLS-DA with S-plot and SUS-plot provides a simplified data analysis method and can be used to identify potentially interesting metabolites. A total of nine metabolites (red dots in Figure 4) were found to be significant in the ecotype as well as in various browning lotus rhizomes in OPLS models. Azelaic acid was upregulated in both OPLS models, whereas (Â±)-aegeline, *N*-feruloyl-3-methoxytyramine, gluconic acid, *N*-trans-feruloyltyramine, p-coumaroyltyramine, and *N*-acetyl-L-phenylalanine were downregulated in both OPLS models. Browning is not obvious in most tropical lotus rhizome samples, and most temperate lotus rhizome samples exhibit different degrees of browning.

4. Discussion and Conclusions

A UPLC-ESI-Q-TOF-HRMS-based untargeted metabolomics approach was used to study the chemical profiles of 14 amino acids, 18 alkaloids, 3 nucleotides, 3 flavonols, 6

phenylpropanoids, and 4 organic acids in *N. nucifera* rhizomes. Thirty-two compounds were identified for the first time in the cultivars of *N. nucifera*. A previous study showed that lotus roots are rich in various compounds including new terpenoids, which were identified in *N. nucifera* rhizome, indicating that the composition of lotus rhizome shows continuous development [16].

PCA is an unsupervised method that is used for model validation, and the OPLS-DA model is used for quality prediction and identification of potential marker metabolites. We observed that biomarker metabolite levels were associated with lotus ecotype and browning. Regarding the relationship between secondary metabolites and browning of sacred lotus rhizome, the levels of (Â±)-aegeline, *N*-feruloyl-3-methoxytyramine, *N*-trans-feruloyltyramine, and dehydrostephanine were positively correlated with browning. However, the levels of (epi) catechin, azelaic acid, and adenosine were negatively correlated with browning. Interestingly, we analyzed the tropical and temperate ecotypes of lotus rhizome samples, which contain most lotus seeds and flowers, and the tropical lotus rhizomes show a lighter brown coloration, whereas most temperate lotus rhizomes are deep brown in color. Temperate lotus sample distribution is extensive, which might affect the construction of the OPLS-DA model, thus making these rhizomes more susceptible to browning. Several studies have reported that phenolic compounds may play important roles in the browning of freshly cut fruits and vegetables and have potential applications in food chemistry; however, there are limited reports on different ecotypes and browning of rhizomes [17, 18]. This indicates the urgent need for a more rational classification method based on ecology. Therefore, our method provides a novel and scientific perspective for classification based on ecology and browning; moreover, it provides useful information and resources for future research on the rational breeding, harvesting, and preservation of lotus rhizomes.

Data Availability

No data were used to support this study.

Disclosure

The funders had no role in study design, data collection and analysis, decision to publish, or preparation of the manuscript.

Conflicts of Interest

The authors declare that they have no conflicts of interest.

Authors' Contributions

Chenyang Hao conceptualized the study, administered the project, and wrote and reviewed the manuscript. Yuetong Yu administered the project, and wrote and reviewed the manuscript. Gangqiang Dong involved in data curation, developed methodology, and wrote and reviewed the manuscript. Xueting Zhang involved in data curation, collected resources, validated the study, and wrote and reviewed the manuscript. Yan Liu and Sha Chen acquired fund, administered the project, and wrote and reviewed the manuscript. Sha Chen is responsible for the integrity of the work as a whole. The authors contributed equally to this manuscript.

Acknowledgments

This work was supported by the Scientific and Technological Innovation Project of China Academy of Chinese Medical Sciences (CACMS innovation fund, CI2021A04515), the Central Public Welfare Research Institutes (ZZ13-YQ-057 and ZXKT20018), and the National Natural Science Foundation of China (32170388).

Supplementary Materials

Table S1: Lotus cultivars used in this manuscript. . (*Supplementary Materials*)

References

[1] G. Chen, M. Zhu, and M. Guo, "Research advances in traditional and modern use of *Nelumbo nucifera*: phytochemicals, health promoting activities and beyond," *Critical Reviews in Food Science and Nutrition*, vol. 59, no. sup1, pp. S189–S209, 2019.

[2] Y. Yi, J. Sun, J. Xie, T. Min, L. M. Wang, and H. X. Wang, "Phenolic profiles and antioxidant activity of lotus root varieties," *Molecules*, vol. 21, no. 7, 863 pages, 2016.

[3] L. Huang, M. Yang, L. Li et al., "Whole genome re-sequencing reveals evolutionary patterns of sacred lotus (*Nelumbo nucifera*)," *Journal of Integrative Plant Biology*, vol. 60, no. 1, pp. 2–15, 2018.

[4] W. Borgi, K. Ghedira, and N. Chouchane, "Antiinflammatory and analgesic activities of Zizyphus lotus root barks," *Fitoterapia*, vol. 78, no. 1, pp. 16–19, 2007.

[5] Y. Jiang, T. B. Ng, C. R. Wang et al., "First isolation of tryptophan from edible lotus (*Nelumbo nucifera* Gaertn) rhizomes and demonstration of its antioxidant effects," *International Journal of Food Sciences & Nutrition*, vol. 61, no. 4, pp. 346–356, 2010.

[6] Y. Tsuruta, K. Nagao, S. Kai et al., "Polyphenolic extract of lotus root (edible rhizome of *Nelumbo nucifera*) alleviates hepatic steatosis in obese diabetic db/db mice," *Lipids in Health and Disease*, vol. 10, no. 1, p. 202, 2011.

[7] M. Yang, L. Zhu, C. Pan et al., "Transcriptomic analysis of the regulation of rhizome formation in temperate and tropical lotus (*Nelumbo nucifera*)," *Scientific Reports*, vol. 5, no. 1, Article ID 13059, 2015.

[8] E. Degl'Innocenti, A. Pardossi, F. Tognoni, and L. Guidi, "Physiological basis of sensitivity to enzymatic browning in 'lettuce', 'escarole' and 'rocket salad'when stored as fresh-cut products," *Food Chemistry*, vol. 104, no. 1, pp. 209–215, 2007.

[9] H. Wang, S. Wang, M. M. Fan, S. H. Zhang, L. L. Sun, and Z. Y. Zhao, "Metabolomic insights into the browning of the peel of bagging 'Rui Xue' apple fruit," *BMC Plant Biology*, vol. 21, no. 1, 209 pages, 2021.

[10] K. Lorenc-Kukuła, R. Amarowicz, J. Oszmiański et al., "Pleiotropic effect of phenolic compounds content increases in transgenic flax plant," *Journal of Agricultural and Food Chemistry*, vol. 53, no. 9, pp. 3685–3692, 2005.

[11] B. D. Oomah, E. O. Kenaschuk, and G. Mazza, "Phenolic acids in flaxseed," *Journal of Agricultural and Food Chemistry*, vol. 43, no. 8, pp. 2016–2019, 1995.

[12] S. S. Rana, R. C. Pradhan, and S. Mishra, "Image analysis to quantify the browning in fresh cut tender jackfruit slices," *Food Chemistry*, vol. 278, pp. 185–189, 2019.

[13] L. Xing, D. Zhang, S. Qi et al., "Transcription profiles reveal the regulatory mechanisms of spur bud changes and flower induction in response to shoot bending in apple (Malus domestica Borkh.)," *Plant Molecular Biology*, vol. 99, no. 1-2, pp. 45–66, 2019.

[14] C. Diez-Simon, R. Mumm, and R. D. Hall, "Mass spectrometry-based metabolomics of volatiles as a new tool for understanding aroma and flavour chemistry in processed food products," *Metabolomics*, vol. 15, no. 3, pp. 41–20, 2019.

[15] S. Chen, Y. Zheng, J. B. Fang, Y. L. Liu, and S. H. Li, "Flavonoids in lotus (Nelumbo) leaves evaluated by HPLC-MSn at the germplasm level," *Food Research International*, vol. 54, no. 1, pp. 796–803, 2013.

[16] P. K. Chaudhuri and D. Singh, "A new triterpenoid from the rhizomes of *Nelumbo nucifera*," *Natural Product Research*, vol. 27, no. 6, pp. 532–536, 2013.

[17] F. F. De Araújo, D. de Paulo Farias, I. A. Neri-Numa, and G. M. Pastore, "Polyphenols and their applications: an approach in food chemistry and innovation potential," *Food Chemistry*, vol. 338, Article ID 127535, 2021.

[18] T. Min, Y. Bao, B. Zhou et al., "Transcription profiles Reveal the regulatory synthesis of phenols during the development of lotus rhizome (*Nelumbo nucifera* Gaertn)," *International Journal of Molecular Sciences*, vol. 20, no. 11, Article ID 2735, 2019.